

Quantum phase transitions in a bidimensional $O(N) \times \mathbb{Z}_2$ scalar field model

Gustavo O. Heymans^a , Marcus Benghi Pinto^b and Rudnei O. Ramos^c

^a*Centro Brasileiro de Pesquisas Físicas, 22290-180 Rio de Janeiro, RJ, Brazil*

^b*Departamento de Física, Universidade Federal de Santa Catarina, 88040-900 Florianópolis, SC, Brazil*

^c*Departamento de Física Teórica, Universidade do Estado do Rio de Janeiro, 20550-013 Rio de Janeiro, RJ, Brazil*

E-mail: olegario@cbpf.br, marcus.benghi@ufsc.br, rudnei@uerj.br

ABSTRACT: We analyze the possible quantum phase transition patterns occurring within the $O(N) \times \mathbb{Z}_2$ scalar multi-field model at vanishing temperatures in $(1 + 1)$ -dimensions. The physical masses associated with the two coupled scalar sectors are evaluated using the loop approximation up to second order. We observe that in the strong coupling regime, the breaking $O(N) \times \mathbb{Z}_2 \rightarrow O(N)$, which is allowed by the Mermin-Wagner-Hohenberg-Coleman theorem, can take place through a second-order phase transition. In order to satisfy this no-go theorem, the $O(N)$ sector must have a finite mass gap for all coupling values, such that conformality is never attained, in opposition to what happens in the simpler \mathbb{Z}_2 version. Our evaluations also show that the sign of the interaction between the two different fields alters the transition pattern in a significant way. These results may be relevant to describe the quantum phase transitions taking place in cold linear systems with competing order parameters. At the same time the super-renormalizable model proposed here can turn out to be useful as a prototype to test resummation techniques as well as non-perturbative methods.

KEYWORDS: quantum phase transition, coupled scalar fields, symmetry breaking

ARXIV EPRINT: [2205.04912 \[hep-th\]](https://arxiv.org/abs/2205.04912)

Contents

1	Introduction	1
2	Warm up: the \mathbb{Z}_2 model	3
2.1	The physical mass	3
3	The $O(N_\phi) \times \mathbb{Z}_2$ model	6
3.1	Physical Masses	7
3.1.1	The subcritical region	8
3.1.2	The supercritical region	8
4	Numerical results	10
4.1	Case $O(N_\phi) \times \mathbb{Z}_2$	10
4.2	Case $\mathbb{Z}_2 \times \mathbb{Z}_2$	14
4.3	Case $O(N_\phi) \times O(N_\chi)$	16
5	Conclusions	16
A	Evaluation of two loop diagrams with mixed propagators	17

1 Introduction

The $\lambda\phi^4$ scalar field model with \mathbb{Z}_2 symmetry in $(1+1)$ -dimensions (ϕ_2^4) is a rather simple quantum field theory model, yet complete enough to illustrate and help to understand many important aspects of much more complicated quantum field theory models. For this reason, it has been extensively considered in the literature (for a far from complete list of references see, e.g., refs. [1–9]). The ϕ_2^4 model describes a simple non-integrable superrenormalizable theory which can display rich phase transition patterns. When the original square mass parameter of the model, m^2 , is positive, the model has a mass gap and remains invariant under the \mathbb{Z}_2 symmetry, as far as one remains within the weak coupling regime. As the strength of the interaction increases, the mass gap decreases until the symmetry gets ultimately broken through a second-order quantum phase transition when a critical coupling value is reached [10, 11]. Since the model’s β -function vanishes at all orders in perturbation theory, it represents a conformal field theory at the critical coupling where it becomes gapless. It then lies within the same universality class as the bidimensional Ising model. These physically appealing characteristics, combined with its simplicity, turn the model into a perfect framework to test how accurately different nonperturbative techniques describe critical parameters associated with the phase transitions.

From the symmetry breaking point of view, it should be recalled that Coleman’s theorem [12] prevents the breaking of a continuous symmetry in $(1+1)$ -dimensions at the

quantum level. When extended to finite temperatures we then refer to the Mermin-Wagner-Hohenberg theorem [13, 14], which states that at finite temperatures, no continuous spontaneous symmetry breaking can occur for $d \leq 3$, where d is the spacetime dimension. Finally, still in the context of low-dimensional systems, Landau's theorem [15] prevents symmetry breaking (be it a continuous or a discrete one in nature) in one-space dimension and at finite temperatures. It is an important consistency check to have these no-go theorems observed in these low-dimensional systems. At the same time, scalar systems with a large symmetry, such as $O(N_\phi) \times O(N_\chi)$ play an important role in a variety of physical situations, including anisotropic antiferromagnets in an external magnetic field [16–18], high- T_c superconductors [19] and possibly even have a role in understanding aspects of extensions of the Standard Model of elementary particles [20–28]. The distinctive transition patterns displayed by these type of models are due to the competition between two coupled fields described by a classical interaction potential of the form [16]

$$V_{\text{int}}(\phi, \chi) = \frac{\lambda_\phi}{4!} \phi^4 + \frac{\lambda_\chi}{4!} \chi^4 + \frac{\lambda}{4} \phi^2 \chi^2, \quad (1.1)$$

where ϕ and χ can be $N_{\phi(\chi)}$ -component fields, $\phi \equiv (\phi_1, \dots, \phi_{N_\phi})$ and $\chi \equiv (\chi_1, \dots, \chi_{N_\chi})$. To avoid a runaway in the interacting potential, eq. (1.1), one needs to enforce boundness from below, which requires the couplings to satisfy $\lambda_\phi, \lambda_\chi \geq 0$ and, if $\lambda < 0$, one needs to further impose $\lambda_\phi \lambda_\chi > 9\lambda^2$. The fact that the interspecies coupling, λ , may be negative can lead to some exotic transition patterns such as *inverse symmetry breaking* as well as *symmetry non-restoration*, which were observed in a seminal paper by Weinberg [29] (in $(3+1)$ -dimensions and at finite temperatures).

As far as planar systems are concerned and in view of the Mermin-Wagner-Hohenberg-Coleman (MWHC) theorem, an interesting possibility has been recently explored in ref. [30] (see also refs. [31, 32] for related works), where the authors analyze the possible phase transition pattern $O(N_\phi) \times \mathbb{Z}_2 \rightarrow O(N)$ occurring in hot planar coupled systems. In the present paper, our aim is to explore the possible (quantum) phase transition patterns exhibited by the same model at vanishing temperatures and in $(1+1)$ -dimensions. The model studied in this paper can also be seen as reminiscent of a two-dimensional XY -Ising model of statistical mechanics (see, e.g., ref. [33] and references therein). The $O(N_\phi) \times \mathbb{Z}_2$ model can also be seen as an extension to lower dimensions, and to the quantum domain, of many previous studies on similar coupled scalar field models [34–45] which were carried out in the presence of a heat bath in $(3+1)$ -dimensions.

The paper is organized as follows. In the next section we review the simplest one-component scalar field case with \mathbb{Z}_2 symmetry. Then, in Sec. 3, we present the $O(N_\phi) \times \mathbb{Z}_2$ model, corresponding to two coupled scalar fields for the general $N_\phi \geq 2$ case. In the same section we evaluate the physical squared masses up to two-loop which represents the first non trivial contribution. Numerical results associated with the phase transition patterns are generated and discussed in Sec. 4. Our conclusions are then presented in Sec. 5. For completeness, some technical details related to the original evaluation of two-loop diagrams with different masses are presented in an Appendix.

2 Warm up: the \mathbb{Z}_2 model

To make the paper self-contained, let us start by reviewing some well known results regarding the \mathbb{Z}_2 model, which is described by the Lagrangian density (in Euclidean space)

$$\mathcal{L} = \frac{1}{2}(\partial_\mu\chi)^2 + \frac{1}{2}m^2\chi^2 + \frac{\lambda}{4!}\chi^4, \quad (2.1)$$

where, in order to investigate the symmetric phase, we take $m^2 > 0$. In (1+1)-dimensions the theory is super-renormalizable and λ has canonical dimensions $[\lambda] = 2$. In this particular case the coupling is finite and, hence, the renormalization group β -function is just $\beta_\lambda = 0$ at all perturbative orders. Regarding the two-point function, the only primitive divergence stems from tadpole (direct) contributions, which do not depend on the external momentum, implying that no wave-function renormalization is needed. Thus, the mass anomalous dimension reads [4]

$$\beta_{m^2} = -\frac{\lambda}{4\pi}. \quad (2.2)$$

2.1 The physical mass

Let us now evaluate the physical square mass for the model (2.1) by considering two regions: the (subcritical) region, where the model is \mathbb{Z}_2 symmetric, and the (supercritical) region, where this symmetry is broken.

The subcritical region ($\lambda < \lambda_c$) is described directly by the Lagrangian density represented by eq. (2.1), from which one may evaluate the physical square mass. Following most applications (e.g., refs. [3, 6, 9]), we will evaluate the pole mass which means that all self-energies are to be evaluated on mass-shell ($p^2 = -m^2$ in Euclidean space). In this case, a semiclassical expansion in loops, to two-loop order yields

$$M^2 = m^2 + \frac{\lambda}{8\pi}L_m - \frac{\lambda^2}{384m^2} - \frac{\lambda^2}{64\pi^2m^2}L_m, \quad (2.3)$$

where L_m is

$$L_m = \ln \frac{\mu^2}{m^2}, \quad (2.4)$$

with μ representing the $\overline{\text{MS}}$ dimensional regularization scale.

After the dynamical symmetry breaking, which is defined by a critical coupling λ_c at which $M^2(\lambda = \lambda_c) = 0$, a nonvanishing vacuum expectation value (VEV) for the field $\bar{\chi}$, develops. One can then perform the usual shift around the new developed VEV: $\chi \rightarrow \chi' = \chi - \bar{\chi}$. After that, the supercritical region ($\lambda > \lambda_c$) is described by the following (Euclidean) Lagrangian density

$$\mathcal{L}' = \frac{1}{2}(\partial_\mu\chi')^2 + \frac{1}{2}\Omega^2(\chi')^2 + \frac{\lambda}{4!}(\chi')^4 + \frac{\lambda}{3!}\bar{\chi}(\chi')^3, \quad (2.5)$$

where

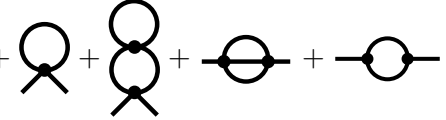
$$\Omega^2 = m^2 + \frac{\lambda}{2}\bar{\chi}^2. \quad (2.6)$$

Note that linear terms do not appear in eq. (2.5) since they all cancel as expected. Hence, at the classical (tree-)level, $\bar{\chi}$ is fixed by

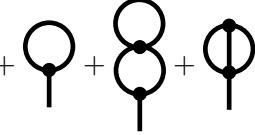
$$m^2\bar{\chi} + \frac{\lambda\bar{\chi}^3}{6} = 0, \quad (2.7)$$

which has $\bar{\chi} = 0$ as its only real solution when $m^2 > 0$. As expected quantum corrections will produce a non-vanishing $\bar{\chi}$ beyond a critical coupling value as we show next.

The contributions up to two-loop order for both the physical square mass and $\Gamma^{(1)}$ now include terms that can be constructed from the tri-linear vertex in eq. (2.5). In this case, the diagrams contributing to the physical square mass and to the tadpole equation $\Gamma^{(1)}$ are, respectively, given by

$$M^2 = \Omega^2 + \text{diagram 1} + \text{diagram 2} + \text{diagram 3} + \text{diagram 4}, \quad (2.8)$$


and

$$\Gamma^{(1)} = -\Omega^2\bar{\chi} + \frac{\lambda\bar{\chi}^3}{3} + \text{diagram 5} + \text{diagram 6} + \text{diagram 7}. \quad (2.9)$$


Evaluating the loop contributions in eqs. (2.8) and (2.9) (on mass-shell) within the $\overline{\text{MS}}$ dimensional regularization scheme, one obtains,

$$M^2 = \Omega^2 + \frac{\lambda}{8\pi}L_\Omega - \frac{\lambda^2}{64\pi^2\Omega^2}L_\Omega - \frac{\lambda^2}{384\Omega^2} - \frac{\lambda^2\bar{\chi}^2}{12\sqrt{3}\Omega^2}, \quad (2.10)$$

while $\bar{\chi}$ is fixed by

$$\Gamma^{(1)} = -\Omega^2\bar{\chi} + \frac{\lambda\bar{\chi}^3}{3} - \frac{\lambda\bar{\chi}}{8\pi}L_\Omega + \frac{\lambda^2\bar{\chi}}{64\pi^2\Omega^2}\bar{\chi}L_\Omega + \frac{\lambda^2\bar{\chi}}{6(8\pi)^2\Omega^2}C_1 \equiv 0, \quad (2.11)$$

where C_1 is a constant given by

$$C_1 = \int_0^\infty dr r K_0(r)^3 \simeq 0.586, \quad (2.12)$$

and L_Ω is defined as

$$L_\Omega = \ln \frac{\mu^2}{\Omega^2}. \quad (2.13)$$

In order to get some numerical results, let us follow other applications [3, 6, 9] by simply setting $\mu = m$. In this case, when in the subcritical region, where $\lambda < \lambda_c$ and $\bar{\chi} = 0$, the pole mass square is given by eq. (2.3), while terms proportional to L_m that appear in there vanish. Hence, tadpoles do not contribute in the subcritical region. By defining the dimensionless coupling $g = \lambda/m^2$, eq. (2.3) can be rewritten in units of m^2 as

$$\frac{M^2}{m^2} = 1 - \frac{g^2}{384}. \quad (2.14)$$

Since $M^2 = 0$ at $g = g_c$, one easily finds $g_c = 8\sqrt{6} \simeq 19.59$, which agrees with the two-loop result found in refs. [3, 9] (once the different parametrizations represented by a $4!$ factor in the definition of the $\lambda\phi^4$ interaction have been adjusted). It should be pointed out that after a resummation including eight-loop perturbative terms [3, 9], one arrives at the much higher value $g_c \sim 67$ (when using our normalization). However, for our present purposes, it is important to notice that the *qualitative* results here obtained, in particular the order of the quantum phase transition taking place when the coupling increases, are not altered by the inclusion of higher order contributions.

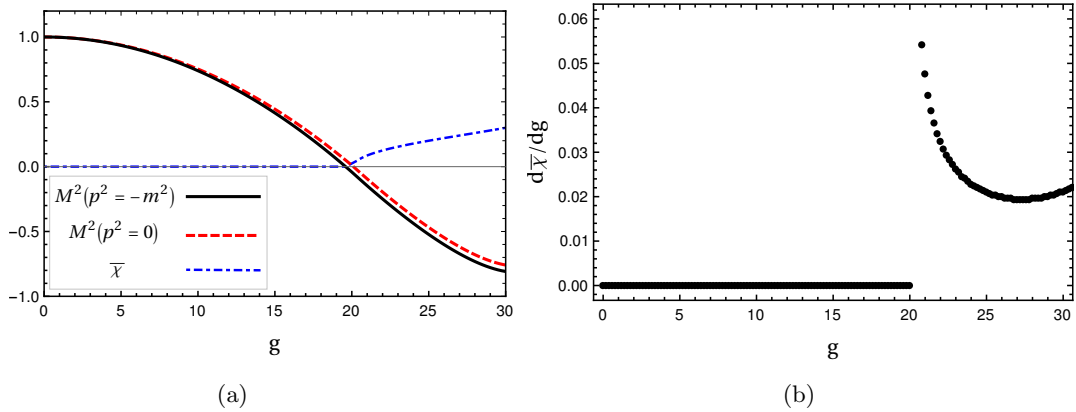


Figure 1. Panel a: M^2/m^2 as a function of g for $M^2(p^2 = -m^2)$ (solid line), $M^2(p^2 = 0)$ (dashed line) and the VEV $\bar{\chi}$ (dash-dotted line). Panel b: the susceptibility $d\bar{\chi}/dg$ as a function of g .

Figure 1(a) shows the dimensionless mass M^2/m^2 and $\bar{\chi}$ as functions of g . It illustrates well the character of the quantum phase transition, as both M^2/m^2 and $\bar{\chi}$ smoothly vanish as the coupling attains its critical value. For completeness, we show in fig. 1(a) both the on-shell square mass $M^2(p^2 = -m^2)$ and also the off-shell one, $M^2(p^2 = 0)$, where the later is given by

$$M^2(p^2 = 0) = m^2 - \frac{\lambda^2}{6(8\pi)^2} C_1. \quad (2.15)$$

At the critical coupling, the \mathbb{Z}_2 symmetry is dynamically broken through a second-order quantum phase transition. Since $\beta_\lambda = 0$ for all coupling values and $M^2(g_c) = 0$, the theory becomes conformal at criticality. Note that within our semiclassical loop expansion evaluation, the exact g_c value depends on whether one uses $M^2(p^2 = -m^2)$ or $M^2(p^2 = 0)$, but the difference turns out to be very small anyway ($g_c = 8\sqrt{6} \simeq 19.6$ for the former and $g_c \simeq 20.1$ for the later). This small quantitative difference can be traced back to the fact that we are not performing any resummations here. Although in this first application to the $O(N_\phi) \times \mathbb{Z}_2$ we shall ignore such small quantitative discrepancies, we do expect that by performing the resummation of high order terms one will eliminate the numerical difference observed here. In the same fig. 1(a) we also show the VEV $\bar{\chi}$, which vanishes at the same point as $M^2(p^2 = 0)$. The fact that both $\bar{\chi}$ and $M^2(p^2 = 0)$ predict the same g_c comes

as no surprise, since both quantities stem from the effective potential (or Landau’s free energy) which generates all 1PI Green’s functions with zero external momentum.

The character of the second-order quantum phase transition can also be verified when computing the VEV susceptibility, $d\bar{\chi}/dg$, whose behavior is shown in fig. 1(b) and which clearly shows the divergence that characterizes a second-order phase transition happening at $g_c \simeq 20$. It is worth to point out that one of the first analysis concerning the quantum phase transition in the model described by eq. (2.1) was performed in ref. [11]. In that reference the Hartree approximation, which is close to a one-loop analysis including only the lowest-order diagram in eq. (2.8), was employed. The result obtained was however a first-order phase transition, which is in contradiction with the Simon-Griffiths theorem [10]. Since the model is in the same universality class as the two-dimensional Ising model, it is then predicted that the transition should be of second-order [10]. Our results, although simply realized within a two-loop approximation, do show consistency with this expectation by correctly predicting the order of the transition.

After having shown that correct *qualitative* results regarding the transition in the case of a single field with a \mathbb{Z}_2 symmetry can be obtained in the two-loop approximation, let us now consider the more involved case of a model with $O(N_\phi) \times \mathbb{Z}_2$ symmetry. As previously discussed, we are aware that a (small) numerical difference related to the exact critical coupling value may arise when the on mass-shell case is not being resummed. Nevertheless, in the sequel, we shall follow refs. [3, 6, 9] among many others defining the critical coupling to be the one at which the on-shell physical mass for a given field vanishes. For our present purposes, there are two main reasons which justify this strategy. Firstly, our main interest here is, from a qualitative point of view, to verify not only the transition patterns allowed by the model, but also to set the necessary conditions on the model parameters such that it will consistently observe the MWHC theorem. Secondly, we expect that the original perturbative evaluation of two-loop terms with on mass-shell contributions to be performed next will help to pave the way for future extensions, including the resummation of higher order terms.

3 The $O(N_\phi) \times \mathbb{Z}_2$ model

Let us now consider a model composed by two different massive scalar fields with one of them (χ) having a single component and the other (ϕ_a) having N_ϕ components. The quartic self-interactions taking place within the different sectors are parametrized by two different couplings, λ_χ and λ_ϕ . The two distinct sectors couple via a bi-quadratic interspecies vertex parametrized by a coupling, λ . Such physical system can be conveniently described by an interaction potential of the form of eq. (1.1) and whose Euclidean Lagrangian density, invariant under $O(N_\phi) \times \mathbb{Z}_2$ global transformations, is given by

$$\begin{aligned} \mathcal{L} = & \frac{1}{2}(\partial_\mu\chi)^2 + \frac{1}{2}m_\chi^2\chi^2 + \frac{\lambda_\chi}{4!}\chi^4 \\ & + \sum_{a=1}^{N_\phi} \left[\frac{1}{2}\partial_\mu\phi_a\partial^\mu\phi_a + \frac{1}{2}m_\phi^2\phi_a\phi_a + \frac{\lambda_\phi}{4!}(\phi_a\phi_a)^2 + \frac{\lambda}{4}\phi_a\phi_a\chi^2 \right]. \end{aligned} \quad (3.1)$$

Owing to the fact that in this application we shall be concerned with the symmetric phase, the model described by eq. (3.1) will be considered only for the case $m_i^2 > 0$ ($i = \chi, \phi$). It should be recalled that our goal is to investigate the dynamical quantum phase transition patterns for the model when it goes from a symmetric to a broken phase, but still observing the MWHC theorem. As in the previous \mathbb{Z}_2 case, the couplings have canonical dimensions $[\lambda_\phi] = [\lambda_\chi] = [\lambda] = 2$, while $\beta_{\lambda_\phi} = \beta_{\lambda_\chi} = \beta_\lambda \equiv 0$. When the interspecies coupling is negative ($\lambda < 0$), the boundness condition for the potential requires that the couplings satisfy the conditions

$$\lambda_\phi > 0, \lambda_\chi > 0 \text{ and } \lambda^2 < \frac{\lambda_\phi \lambda_\chi}{9}. \quad (3.2)$$

Since the model described by eq. (3.1) has not been previously considered in $(1+1)$ -dimensions, let us briefly discuss its renormalizability as well as renormalization group properties. Just like the related \mathbb{Z}_2 version the extended $O(N_\phi) \times \mathbb{Z}_2$ version is also super renormalizable in $(1+1)$ -dimensions and the only primitive divergences stem from the one-loop contributions to the self-energies Σ_i ($i = \chi, \phi$). Computing the physical masses, $M_i^2 = m_i^2 + \Sigma_i$, to one-loop order within the $\overline{\text{MS}}$ dimensional regularization scheme, one obtains

$$M_\chi^2 = m_\chi^2 + \frac{\lambda_\chi}{8\pi} \left(\frac{1}{\epsilon} + L_{m_\chi} \right) + \frac{\lambda N_\phi}{8\pi} \left(\frac{1}{\epsilon} + L_{m_\phi} \right) + \delta m_\chi^2, \quad (3.3)$$

and

$$M_\phi^2 = m_\phi^2 + \frac{\lambda_\phi(N_\phi + 2)}{24\pi} \left(\frac{1}{\epsilon} + L_{m_\phi} \right) + \frac{\lambda}{8\pi} \left(\frac{1}{\epsilon} + L_{m_\chi} \right) + \delta m_\phi^2, \quad (3.4)$$

where

$$L_{m_i} \equiv \ln \frac{\mu^2}{m_i^2}. \quad (3.5)$$

The contributions δm_i^2 ($i = \chi, \phi$) represent mass counterterms whose sole purpose is to remove the poles. After renormalization, each finite physical mass must satisfy the Callan-Symanzik equation,

$$(\mu \partial_\mu + \beta_{m_i^2} \partial_{m_i^2} + \beta_{m_j^2} \partial_{m_j^2}) M_i^2 = 0, \quad (3.6)$$

from which one obtains

$$\beta_{m_\chi} = -\frac{1}{4\pi} (\lambda_\chi + \lambda N_\phi), \quad (3.7)$$

and

$$\beta_{m_\phi} = -\frac{1}{4\pi} \left[\lambda_\phi \frac{(N_\phi + 2)}{3} + \lambda \right]. \quad (3.8)$$

The above equations generalize the well known \mathbb{Z}_2 result given by eq. (2.2) to the present case of a $O(N_\phi) \times \mathbb{Z}_2$ invariant model.

3.1 Physical Masses

Let us now evaluate the (on mass-shell) physical square masses considering two regions: (a) the (subcritical) region, where the model is still $O(N_\phi) \times \mathbb{Z}_2$ symmetric and, (b) the (supercritical) region, where the \mathbb{Z}_2 symmetry associated with the χ sector has been dynamically broken by radiative corrections. Note that a third (hypercritical) region, where

the full $O(N_\phi) \times \mathbb{Z}_2$ symmetry could be eventually broken, is excluded by the MWHC theorem.

3.1.1 The subcritical region

For the sake of generality, let us consider the case $m_\phi \neq m_\chi$. Up to two loops the physical masses receive the following contributions:

$$M_i^2 = m_i^2 + \text{diagram 1} + \text{diagram 2} + \text{diagram 3} + \text{diagram 4} + \text{diagram 5} + \text{diagram 6} + \text{diagram 7} + \text{diagram 8} + \text{diagram 9}. \quad (3.9)$$

Performing the evaluations (see appendix A for some of the technical details) within the $\overline{\text{MS}}$ dimensional regularization scheme, one obtains the finite result

$$\begin{aligned} M_i^2 = & m_i^2 + \frac{\lambda_i(N_i+2)}{24\pi} L_{m_i} + \frac{N_j\lambda}{8\pi} L_{m_j} - \frac{(N_i+2)^2\lambda_i^2}{36(4\pi)^2 m_i^2} L_{m_i} - \frac{(N_i+2)N_j\lambda_i\lambda}{12(4\pi)^2 m_i^2} L_{m_j} \\ & - \frac{(N_j+2)N_j\lambda_j\lambda}{12(4\pi)^2 m_j^2} L_{m_j} - \frac{N_i N_j \lambda^2}{4(4\pi)^2 m_j^2} L_{m_i} - \frac{(N_i+2)\lambda_i^2}{1152 m_i^2} \\ & - \frac{N_j\lambda^2}{4(4\pi)^2 m_i m_j} \left[\pi^2 - 4 \tanh^{-1} \left(\frac{m_j}{m_i} \right) \ln \left(\frac{m_i}{m_j} \right) - \frac{m_j}{m_i} \Phi \left(\frac{m_j^2}{m_i^2}, 2, \frac{1}{2} \right) \right], \end{aligned} \quad (3.10)$$

where $i \neq j = \phi, \chi$ and $N_\chi = 1$. In the above equation $\Phi(z, s, a)$ represents the Lerch transcendent function [46].

3.1.2 The supercritical region

When the only phase transition allowed by the MWHC theorem, i.e., $O(N_\phi) \times \mathbb{Z}_2 \rightarrow O(N_\phi)$, takes place within the χ sector, the Lagrangian density needs to be written in terms of the shifted field, $\chi' = \chi - \bar{\chi}$. One then arrives at

$$\begin{aligned} \mathcal{L}' = & \frac{1}{2} \partial_\mu \phi_a \partial^\mu \phi_a + \frac{1}{2} \Omega_\phi^2 \phi_a \phi_a + \frac{\lambda_\phi}{4!} (\phi_a \phi_a)^2 + \frac{1}{2} (\partial_\mu \chi')^2 + \frac{1}{2} \Omega_\chi^2 (\chi')^2 + \frac{\lambda_\chi}{4!} (\chi')^4 + \frac{\lambda}{4} \phi_a \phi_a (\chi')^2 \\ & + \frac{\lambda_\chi}{3!} \bar{\chi} (\chi')^3 + \frac{\lambda}{2} \bar{\chi} \phi_a \phi_a \chi', \end{aligned} \quad (3.11)$$

where

$$\Omega_\phi^2 = m_\phi^2 + \frac{\lambda}{2} \bar{\chi}^2, \quad (3.12)$$

$$\Omega_\chi^2 = m_\chi^2 + \frac{\lambda_\chi}{2} \bar{\chi}^2. \quad (3.13)$$

To obtain the tadpole equation for $\Gamma^{(1)}$ up to two-loop order, one needs to evaluate the contributions shown below:

$$\Gamma^{(1)} = -\bar{\chi} m_\chi^2 - \frac{\lambda_\chi}{6} \bar{\chi}^3 + \text{diagram 1} + \text{diagram 2} + \text{diagram 3} + \text{diagram 4} + \text{diagram 5} + \text{diagram 6} + \text{diagram 7} + \text{diagram 8}. \quad (3.14)$$

Within the supercritical region the masses also receive new contributions from the trilinear vertex which depends on the VEV, $\bar{\chi}$. This leads to additional terms contributing to eq. (3.9) which, for the χ and ϕ fields respectively, yields

$$M_\chi^2 = \Omega_\chi^2 + \text{[diagrams]} \quad (3.15)$$

and

$$M_\phi^2 = \Omega_\phi^2 + \text{[diagrams]} \quad (3.16)$$

Then, the finite results for the masses in eqs. (3.15) and (3.16) read

$$M_\chi^2 = \Omega_\chi^2 + \frac{\lambda_\chi}{8\pi} L_{\Omega_\chi} + \frac{N_\phi \lambda}{8\pi} L_{\Omega_\phi} - \frac{\lambda_\chi^2}{(8\pi)^2 \Omega_\chi^2} L_{\Omega_\chi} - \frac{N_\phi \lambda_\chi \lambda}{(8\pi)^2 \Omega_\chi^2} L_{\Omega_\phi} - \frac{(N_\phi + 2) N_\phi \lambda_\phi \lambda}{3(8\pi)^2 \Omega_\phi^2} L_{\Omega_\phi} - \frac{N_\phi \lambda^2}{(8\pi)^2 \Omega_\phi^2} L_{\Omega_\chi} - \frac{\lambda_\chi^2}{384 \Omega_\chi^2} - \frac{N_\phi \lambda^2}{(8\pi)^2 \sqrt{\Omega_\chi^2 \Omega_\phi^2}} \left[\pi^2 - 2 \operatorname{arctanh} \left(\sqrt{\frac{\Omega_\phi^2}{\Omega_\chi^2}} \right) \ln \left(\frac{\Omega_\phi^2}{\Omega_\chi^2} \right) - \sqrt{\frac{\Omega_\phi^2}{\Omega_\chi^2}} \Phi \left(\frac{\Omega_\phi^2}{\Omega_\chi^2}, 2, \frac{1}{2} \right) \right] - \frac{\lambda_\chi^2 \bar{\chi}^2}{12 \sqrt{3} \Omega_\chi^2} - \frac{N_\phi \lambda^2 \sqrt{\pi} \bar{\chi}^2}{8 \Omega_\chi^2} G_{12}^{21} \left(\frac{4 \Omega_\phi^2}{\Omega_\chi^2} \middle| \begin{matrix} 0, -1/2, 1/2 \\ 0, 0, -1/2 \end{matrix} \right), \quad (3.17)$$

where $G_{12}^{21} \left(z \middle| \begin{matrix} 0, -1/2, 1/2 \\ 0, 0, -1/2 \end{matrix} \right)$ represents the Meijer-G function [46] and

$$M_\phi^2 = \Omega_\phi^2 + \frac{(N_\phi + 2) \lambda_\phi}{24\pi} L_{\Omega_\phi} + \frac{\lambda}{8\pi} L_{\Omega_\chi} - \frac{(N_\phi + 2)^2 \lambda_\phi^2}{9(8\pi)^2 \Omega_\phi^2} L_{\Omega_\phi} - \frac{(N_\phi + 2) \lambda_\phi \lambda}{3(8\pi)^2 \Omega_\phi^2} L_{\Omega_\chi} - \frac{\lambda_\chi \lambda}{(8\pi)^2 \Omega_\chi^2} L_{\Omega_\chi} - \frac{N_\phi \lambda^2}{4(4\pi)^2 \Omega_\chi^2} L_{\Omega_\phi} - \frac{(N_\phi + 2) \lambda_\phi^2}{1152 \Omega_\phi^2} - \frac{\lambda^2}{(8\pi)^2 \sqrt{\Omega_\phi^2 \Omega_\chi^2}} \left[\pi^2 - 2 \operatorname{arctanh} \left(\sqrt{\frac{\Omega_\chi^2}{\Omega_\phi^2}} \right) \ln \left(\frac{\Omega_\chi^2}{\Omega_\phi^2} \right) - \sqrt{\frac{\Omega_\chi^2}{\Omega_\phi^2}} \Phi \left(\frac{\Omega_\chi^2}{\Omega_\phi^2}, 2, \frac{1}{2} \right) \right] - \frac{\lambda^2 \bar{\chi}^2}{2\pi \sqrt{\Omega_\phi^2 \Omega_\chi^2} \sqrt{4 - \frac{\Omega_\chi^2}{\Omega_\phi^2}}} \operatorname{arcsec} \left(\sqrt{\frac{4 \Omega_\phi^2}{\Omega_\chi^2}} \right), \quad (3.18)$$

where

$$L_{\Omega_i} = \ln \frac{\mu^2}{\Omega_i^2}. \quad (3.19)$$

As before, $\bar{\chi}$ is determined from $\Gamma^{(1)} = 0$, where

$$\begin{aligned} \Gamma^{(1)} = & -\bar{\chi}m_\chi^2 - \frac{\lambda_\chi \bar{\chi}^3}{6} - \frac{\lambda_\chi \bar{\chi}}{8\pi} L_{\Omega_\chi} - \frac{N_\phi \lambda \bar{\chi}}{8\pi} L_{\Omega_\phi} \\ & + \frac{\lambda_\chi^2 \bar{\chi}}{(8\pi)^2 \Omega_\chi^2} L_{\Omega_\chi} + \frac{N_\phi \lambda^2 \bar{\chi}}{(8\pi)^2 \Omega_\phi^2} L_{\Omega_\chi} + \frac{N_\phi (N_\phi + 2) \lambda_\phi \lambda \bar{\chi}}{192\pi^2 \Omega_\phi^2} L_{\Omega_\phi} + \frac{N_\phi \lambda_\chi \lambda \bar{\chi}}{(8\pi)^2 \Omega_\chi^2} L_{\Omega_\phi} \\ & + \frac{\lambda_\chi^2 \bar{\chi}}{6(8\pi)^2 \Omega_\phi^2} C_1 + \frac{N_\phi \lambda^2 \bar{\chi}}{16\pi^{3/2} \Omega_\chi^2} G_{10}^{32} \left(\begin{array}{c} 4\Omega_\phi^2 \\ \Omega_\chi^2 \end{array} \middle| \begin{array}{c} 0, 0, 1/2 \\ 0, 0, 0, - \end{array} \right). \end{aligned} \quad (3.20)$$

4 Numerical results

For numerical evaluations we take $m_\chi = m_\phi \equiv m$, while defining the dimensionless couplings $g = \text{sgn}(\lambda)|\lambda|/m^2$, and $g_i = \lambda_i/m^2$, $i = \phi, \chi$. Then, following most applications to the \mathbb{Z}_2 case, we set¹ the $\overline{\text{MS}}$ scale to $\mu = m$. With this particular choice, all tadpole diagrams, which are proportional to L_{m_i} , vanish within the subcritical region. At the same time, within the supercritical region, the logarithmic terms contained in the masses and tadpole contributions can be explicitly written as

$$L_{\Omega_\chi} = \ln \left(\frac{1}{1 + g_\chi \bar{\chi}^2/2} \right), \quad (4.1)$$

and

$$L_{\Omega_\phi} = \ln \left(\frac{1}{1 + g \bar{\chi}^2/2} \right). \quad (4.2)$$

4.1 Case $O(N_\phi) \times \mathbb{Z}_2$

Applying the definitions set above for the subcritical masses described by eq. (3.10), one obtains

$$\frac{M_\chi^2}{m^2} = 1 - \frac{g_\chi^2}{384} - \frac{g^2}{128} N_\phi, \quad (4.3)$$

and

$$\frac{M_\phi^2}{m^2} = 1 - \frac{g_\phi^2 (N_\phi + 2)}{384} - \frac{g^2}{128}. \quad (4.4)$$

At first glance, one could expect that the symmetry would be ultimately broken in both channels, however, this is not guaranteed. The reason is that after the breaking in one direction (e.g., χ), the masses begin to depend explicitly on the VEV $\bar{\chi}$, as dictated by eqs. (3.17) and (3.18), such that the supercritical region may be appropriately described as already mentioned. In this case, M_ϕ^2 will be affected by $\bar{\chi}$ as well as by the sign of the interspecies coupling g . In order to investigate whether there is a possibility that the MWHC theorem will not be violated, it is instructive to analyze the phase diagram

¹Other scales can be chosen in accordance with the masses $m_i(\mu)$ running, which is dictated by eqs. (3.7) and (3.8).

boundaries on the $(g_{i,c}, g)$ -plane. From eqs. (4.3) and (4.4), we can readily determine the critical couplings $g_{\chi,c}$ and $g_{\phi,c}$ as functions of g ,

$$g_{\chi,c}(g) = 8\sqrt{6} \left(1 - \frac{g^2}{128} N_\phi\right)^{1/2}, \quad (4.5)$$

and

$$g_{\phi,c}(g) = 8\sqrt{6} \left(\frac{3}{N_\phi + 2}\right)^{1/2} \left(1 - \frac{g^2}{128}\right)^{1/2}. \quad (4.6)$$

Imposing that the breaking occurs first in the direction of the χ field, i.e., $g_{\chi,c}(g) < g_{\phi,c}(g)$, this implies that g must satisfy the condition

$$g > 8\sqrt{\frac{2}{N_\phi + 3}}. \quad (4.7)$$

On the other hand, for lower values of g , one has instead that $g_{\phi,c} < g_{\chi,c}$, which means that the $O(N_\phi)$ symmetry is broken first than the \mathbb{Z}_2 one violating the MWHC theorem within this weak coupling regime. As g increases, $g_{\chi,c}$ approaches $g_{\phi,c}$ until they merge at the crossing value $g = g_*$ given by

$$g_* = 8\sqrt{\frac{2}{N_\phi + 3}}. \quad (4.8)$$

After this crossing point we have $g_{\chi,c} > g_{\phi,c}$ implying that the \mathbb{Z}_2 symmetry breaking (in the χ -direction) occurs first. Once the \mathbb{Z}_2 symmetry has been broken, the χ field acquires a VEV $\bar{\chi}$ and one must use eqs. (3.18) and (3.20) for M_ϕ^2 and $\bar{\chi}$, respectively. Now, the condition $M_\phi^2 = 0$ determines a new value for $g_{\phi,c}$ which allows us to determine which region of the parameters space is excluded by the MWHC theorem. In this situation one may use the two coupled eqs. (3.18) and (3.20) to determine the two unknowns $g_{\phi,c}$ and $\bar{\chi}$ for each g value. Since both equations also depend on g_χ , one can set $g_\chi = 9g^2/g_\phi$, which apart from being the threshold for boundness, it is also exactly satisfied at the crossing point when $g_{\chi,c}(g_*) = g_{\phi,c}(g_*)$.

In fig. 2 we display the corresponding phase diagrams in the space of the coupling constants. The case $g > 0$, shown in fig. 2(a), illustrates that it is possible to preserve the $O(N_\phi)$ symmetry at arbitrarily large g values provided that $g_\phi < 3g$. The case $g < 0$, shown in fig. 2(b), describes a completely different scenario since the theory is only bounded in the interval $[0, g_*)$ in which the MWHC theorem is violated. To carry out the analysis starting exactly at the unstable g_* , as we did in the $g > 0$ case, requires setting $g_\chi = 9g^2/g_\phi$, which violates the boundness condition. As a consequence, the whole region $g \geq g_*$ is forbidden. This means that when the couplings are independent and the interspecies interaction is repulsive ($g < 0$) the symmetry breaking pattern $O(N_\phi) \times \mathbb{Z}_2 \rightarrow O(N_\phi)$ cannot take place in any regime. Finally, we remark that $g_* \rightarrow 0$ when $N_\phi \rightarrow \infty$ so that the MWHC theorem

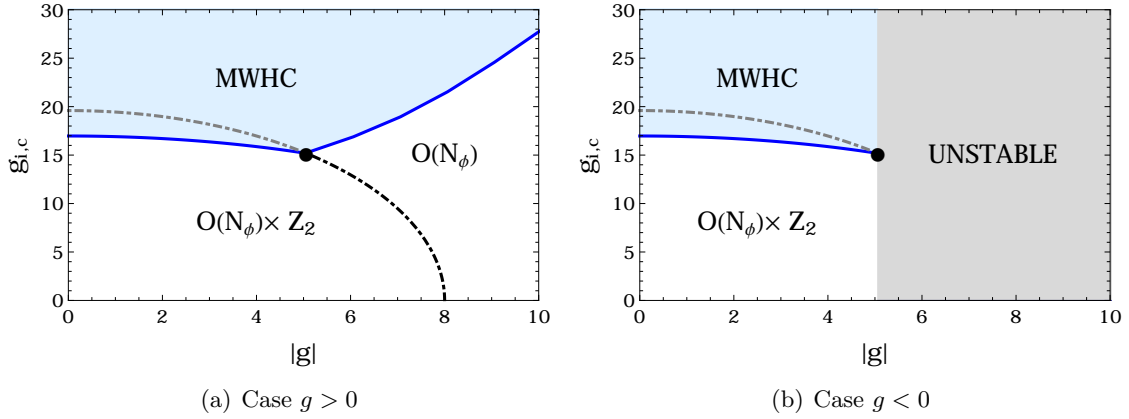


Figure 2. Phase diagrams on the $(g_{i,c}, g)$ plane for $g > 0$ (panel a) and $g < 0$ (panel b). The continuous line represents $g_{\phi,c}$ and the dash-dotted line represents $g_{\chi,c}$. In both panels the region labelled MWHC indicates where the $O(N_\phi)$ symmetry is broken and thus excluded by the no-go theorem. Within the region labelled *UNSTABLE* in the right panel the boundness condition that applies to the case $g < 0$ is not observed. We have taken in this example $N_\phi = 2$, which gives $g_* = 8\sqrt{2/5} \simeq 5.05$.

covers a region of smaller g values. In the case of $g > 0$ this means that the breaking $O(N_\phi) \times \mathbb{Z}_2 \rightarrow O(N_\phi)$ can take place at weaker couplings. On the other hand, when $g < 0$, the first boundary of the unstable region will start at a smaller g_* value compensating the shrinkage of the MWHC region and forbidding any transition to take place, just like in the $N_\phi = 2$ example shown in fig. 2.

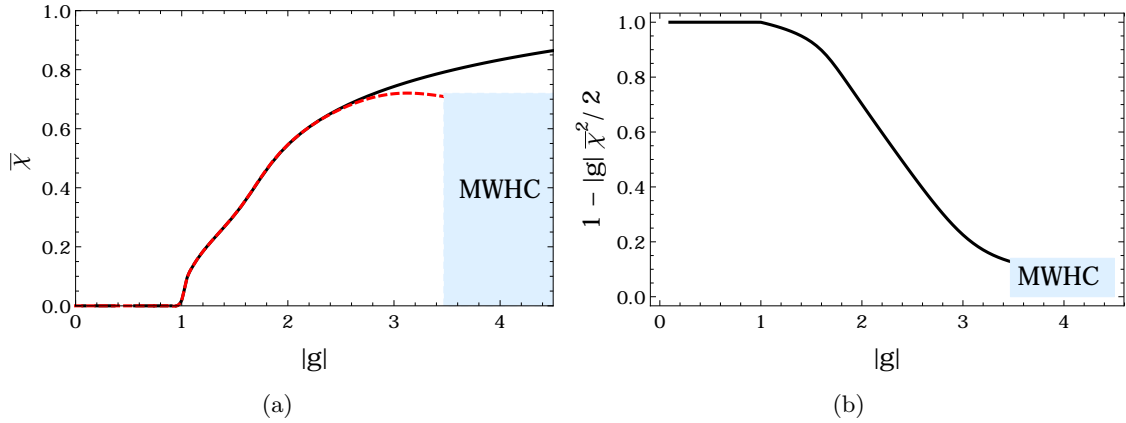


Figure 3. Panel a: The VEV of the χ field, $\bar{\chi}$, as a function of $|g|$ for $g > 0$ (solid line) and for $g < 0$ (dashed line). Panel b: Ω_χ^2/m^2 as a function of $|g|$ in the case of $g < 0$. The parameters chosen in both plots are $N_\phi = 2$ while the self-couplings are given by $g_i(g) = k_i|g|$, with $k_\chi = 20$ and $k_\phi = 0.5$.

It is also useful to explore alternative scenarios where the self-couplings g_ϕ and g_χ are

not independent, but might be expressed, e.g., as a function of the interspecies coupling g . The simplest case is just when the relation between the couplings is of the form $g_i(g) = k_i|g|$, where the proportionality factor k_i represents some positive constant. In this case, the breaking of the \mathbb{Z}_2 symmetry will certainly occur first if the self-interactions within the χ sector are much stronger than the ones occurring within the ϕ counterpart, i.e., $k_\chi \gg k_\phi$. To treat the case where the interspecies coupling is repulsive ($g < 0$), one must further require that $k_\chi k_\phi > 9$. To investigate the different possible symmetry breaking patterns, let us suppose for illustration purposes that $k_\chi = 20$ and $k_\phi = 0.5$ as a representative example of parameters choice. In this case, the requirement that the \mathbb{Z}_2 symmetry breaks first is satisfied together with the boundness condition. Then, substituting $g_\chi(g)$ and $g_\phi(g)$ respectively into eqs. (4.5) and (4.6) one finds that, as expected, the first breaking occurs in the χ -direction at $g_c = 8\sqrt{3/203} \simeq 0.97$. To investigate an eventual breaking in the ϕ -direction one needs to consider eqs. (3.18) and (3.20) within the supercritical region. After imposing χ to be gapless, i.e., $M_\chi^2 = 0$, one then solves the two coupled eqs. (3.18) and (3.20) to find the two unknowns $|g_c|$ and $\bar{\chi}$. Starting with the case $g > 0$, one cannot find a positive solution for $|g_c|$ and $\bar{\chi}$, whereas when $g < 0$, one finds $|g_c| \simeq 3.47$ and $\bar{\chi} \simeq 0.70$. These results corroborate the fact that the MWHC theorem is respected (violated) when the interspecies coupling is attractive (repulsive). Here, it becomes important to make a digression. Note that within the supercritical region the VEV ($\bar{\chi} \neq 0$) enters quantities such as $\Omega_\phi^2/m^2 = 1 + \text{sgn}(g)|g|\bar{\chi}^2/2$, which becomes complex if $\text{sgn}(g) = -$ and $g\bar{\chi}^2 > 2$. The situation is illustrated by fig. 3(a), which shows $\bar{\chi}$ as a function of $|g|$ for both cases of $\text{sgn}(g) = \pm$, and by fig. 3(b), which shows the quantity $\Omega_\chi^2/m^2 = 1 - |g|\bar{\chi}^2/2$ also as a function of $|g|$ when $\text{sgn}(g) = -$. These results reassure us that $\Omega_\phi^2 \in \mathbb{R}$ before the forbidden hypercritical region is reached (up to the point where the curves reach the MWHC region).

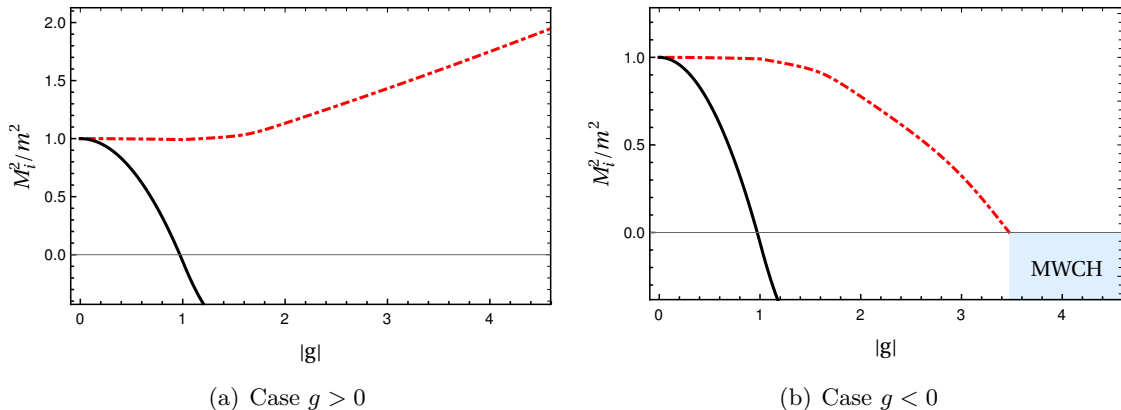


Figure 4. The pole masses as functions of $|g|$. The solid line shows M_χ^2/m^2 and the dash-dotted line represents M_ϕ^2/m^2 . The same parametrization considered in fig. 3 is used here.

To get further insight in this case where $g_i = k_i|g|$, let us investigate the pole masses $M_i^2(g)$ considering $\text{sgn}(g) = \pm$ for the case $O(N_\phi) \times \mathbb{Z}_2$, with $N_\phi = 2$. The results for this

example are shown in fig. 4. They indicate that when $g > 0$ the ϕ field does not become gapless as g increases, then respecting the MWHC theorem at arbitrarily high g values. On the other hand, when $g < 0$, fig. 4(b) shows that at $|g_c| \simeq 3.47$ the MWHC region will be reached and, hence, only the regimes of weak to moderate coupling values ($|g| < |g_c|$) can be explored.

In connection to the above results, it is worth to comment on the validity of the results in the supercritical regime. Even though we do not make use here of a perturbative expansion, but a loop one, we recall the subtleties of going beyond the gapless phase, which is intrinsic to perturbation theory [4]. At the critical point, where $M_\chi^2(g = g_c) = 0$, singularities are expected and $M_\chi^2(g)$ could have different branches. It is not obvious that the analytic continuation given by perturbation theory gives the correct branch. Therefore, following refs. [3, 4], we refrain from investigating the detailed behavior of $M_\chi^2 < 0$. For our purposes, this course of action is totally justifiable since after the first breaking the order parameter of interest, namely M_ϕ^2 , is affected by $\bar{\chi} \neq 0$ rather than by $M_\chi^2 < 0$.

4.2 Case $\mathbb{Z}_2 \times \mathbb{Z}_2$

For completeness, let us now examine the case where $N_\phi = 1$ and, hence, the model is $\mathbb{Z}_2 \times \mathbb{Z}_2$ symmetric. Since now only discrete symmetries are involved, the MWHC theorem does not apply. From eqs. (4.5) and (4.6), one can see that in this case the (degenerate) critical couplings are given by

$$g_{i,c}(g) = 8\sqrt{6} \left(1 - \frac{g^2}{128}\right)^{1/2}, \quad (4.9)$$

which indicates that when the couplings are independent, the transition $\mathbb{Z}_2 \times \mathbb{Z}_2 \rightarrow 1$ always happens at once.

In fig. 5(a) we show the resulting phase diagram for $g > 0$. It can be seen that the symmetry will always be completely broken when the strong coupling regime is attained. The case $g < 0$ requires extra care because although eq. (4.9) does not depend on the sign of g , the boundness condition still has to be satisfied. Then, with $g_{\chi,c} = g_{\phi,c} \equiv g_{i,c}$, one must further impose $g_{i,c} > 3g$. The phase diagram in this case is displayed in fig. 5(b). It is important to remark that in both cases the theory is conformal along the allowed (coincident) transition lines.

Next, for illustration purposes, let us set $g_\chi = 20|g|$ and $g_\phi = 0.5|g|$ in order to perform the same type of analysis carried out in the previous subsection and where the case $O(N_\phi) \times \mathbb{Z}_2$ was considered. Since now the MWHC theorem does not apply and the boundness condition is enforced by construction, one can expect, based on the results obtained for the $O(N_\phi) \times \mathbb{Z}_2$ case, that two scenarios will emerge: i) when $g > 0$ the transition pattern will be $\mathbb{Z}_2 \times \mathbb{Z}_2 \rightarrow \mathbb{Z}_2$ and ii) when $g < 0$ one expects to also reach the

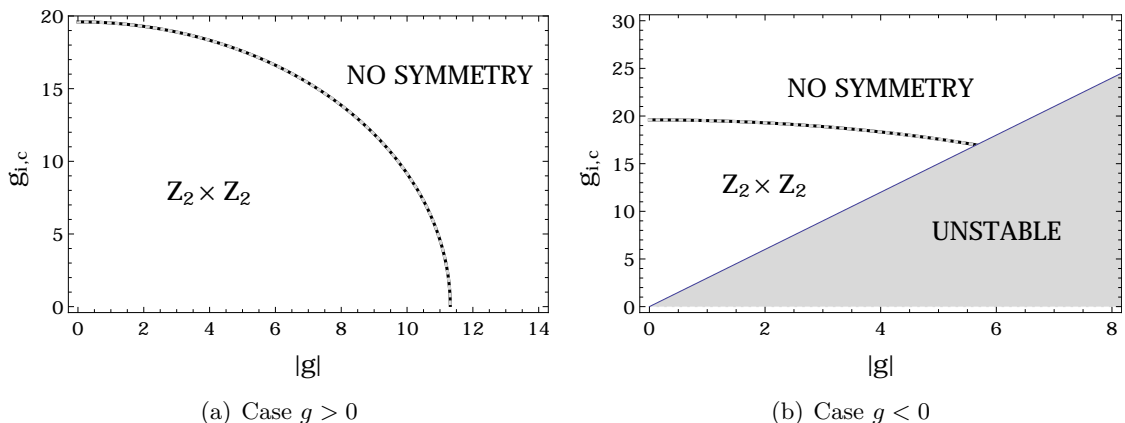


Figure 5. Phase diagrams in the $g_{i,c}, g$ plane for $g > 0$ (panel a) and $g < 0$ (panel b) for the $\mathbb{Z}_2 \times \mathbb{Z}_2$ symmetric model. The region labelled *UNSTABLE* indicates where the boundness condition $g_\phi g_\chi > 9g^2$ is not obeyed. The light continuous line representing $g_{\chi,c}$ and the dark dotted line representing $g_{\phi,c}$ coincide indicating that conformability has been attained at the transition boundary.

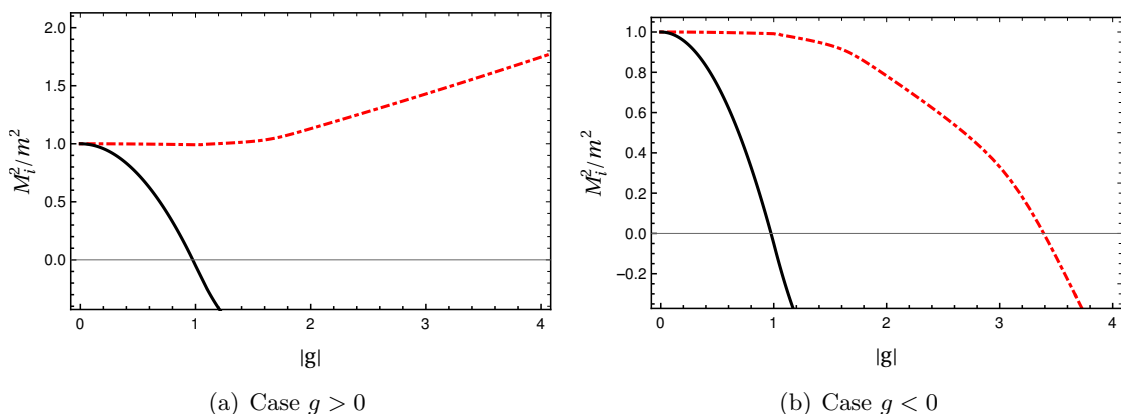


Figure 6. The pole masses as a function of $|g|$ for the $\mathbb{Z}_2 \times \mathbb{Z}_2$ symmetric model. The solid line shows M_χ^2/m^2 and the dash-dotted line is for M_ϕ^2/m^2 . The parameters are chosen such as $g_\chi = 20|g|$ and $g_\phi = 0.5|g|$ in this example.

hypercritical region, where the remaining \mathbb{Z}_2 symmetry, associated with the ϕ sector, will be ultimately broken. As fig. 6 illustrates, these symmetry breaking patterns are indeed exactly reproduced according to whether $g > 0$ (fig. 6(a)) or $g < 0$ (fig. 6(b)). It is important to remark that although both sectors, χ and ϕ , become gapless in the $\mathbb{Z}_2 \times \mathbb{Z}_2$ case when $g < 0$, this does not automatically imply that the theory will be conformal. As fig. 6 reveals, when $g_i = k_i|g|$ and $k_\chi \neq k_\phi$, the two transitions happen at different coupling values. On the other hand, as already discussed, when the couplings are independent and the tree-level masses are degenerate the theory is completely gapless and, therefore, conformal along the whole transition line displayed in fig. 5.

4.3 Case $O(N_\phi) \times O(N_\chi)$

Before closing this section, let us comment on the situation for the $O(N_\phi) \times O(N_\chi)$ case with $N_i \geq 2$. In this scenario, the Lagrangian density can be trivially modified with χ becoming a N_χ -component field. In the subcritical region, one would then obtain the following masses at two-loop order,

$$\frac{M_i^2}{m^2} = 1 - \frac{g_i^2}{384} \frac{(N_i + 2)}{3} - \frac{g^2}{128} N_j \quad (i, j = \chi, \phi), \quad (4.10)$$

which is the generalization of eqs. (4.5) and (4.6). It then happens that the MWHC theorem would be unavoidably violated at

$$g_{i,c}(g) = 8\sqrt{6} \left(\frac{3}{N_i + 2} \right)^{1/2} \left(1 - \frac{g^2}{128} N_j \right)^{1/2}. \quad (4.11)$$

Therefore, requiring that none of the continuous symmetries in the case $O(N_\phi) \times O(N_\chi)$ be broken, which would violate the MWHC theorem, sets a bound for the allowed coupling values. Namely, they must be sufficiently weak in order to guarantee $M_i^2 > 0$. On the other hand, it is worth also recalling that when either $N_\phi \rightarrow \infty$ or $N_\chi \rightarrow \infty$, or both are taken in the large- N limit, Coleman's theorem no longer applies in that specific field direction [47, 48]. Finally, when stable point-like topological defects can be formed in two dimensional systems with a spontaneously broken symmetry at zero temperature, we can have a Berezinskii-Kosterlitz-Thouless (BKT) phase transition [49, 50]. In this case, a phase transition can occur, yet with no symmetry being truly broken. This is also a situation where the no-go theorems regarding the breaking of continuous symmetries at low dimensions can be evaded. Although this situation could arise in the model studied here, which can admit the formation of global topological nontrivial solutions, its investigation is far beyond the scope of the present work.

5 Conclusions

We have analyzed the possible phase transition patterns that may occur within a bidimensional scalar multi-field model with $O(N_\phi) \times \mathbb{Z}_2$ symmetry. Using the semiclassical loop approximation to next-to-leading order, we have shown that the breaking $O(N_\phi) \times \mathbb{Z}_2 \rightarrow O(N_\phi)$, which respects the Mermin-Wagner-Hohenberg-Coleman no-go theorem may occur. The transition shows to be of the second kind as in the simpler \mathbb{Z}_2 version. We have also obtained which conditions the model parameters need to satisfy in order to observe the no-go theorem. For instance, when the couplings are independent and the interspecies coupling g is attractive ($g > 0$), strong couplings are allowed, provided that \mathbb{Z}_2 breaks first and that $g_\phi < 3g$. On the other hand, when the couplings are independent and the interspecies coupling is repulsive ($g < 0$), the MWHC theorem together with the stability condition for the potential, restricts the couplings to the weak regime. By taking for example the couplings related through a linear relation, $g_i = k_i|g|$ with $k_\chi \gg k_\phi$ and $g > 0$ the model allows for all values of g , while remaining consistent with the MWHC theorem. On the other hand, if $g < 0$, only weak and moderate coupling values are allowed.

We have also analyzed the $\mathbb{Z}_2 \times \mathbb{Z}_2$ special case which is not tied up by the MWHC theorem. In this case, the allowed parameter region is solely restricted when the inter-species coupling is repulsive, enforcing the stability condition to be observed. When the couplings are independent, both (χ and ϕ) sectors become gapless at once, implying total conformability along the critical transition line. Finally, we have also discussed the case with $O(N_\phi) \times O(N_\chi)$ symmetry. In this case, for any sign of the interspecies coupling, the MWHC theorem restricts the couplings to the weak regime only.

In all the cases analyzed, our results indicate that the sign of the interspecies coupling (attractive/repulsive) can alter the transition pattern in a significant way. The results obtained here may be relevant to describe the quantum phase transitions taking place in cold linear systems with competing order parameters, where descriptions in terms of scalar multi-field systems are used. Eventually, our model could also serve to investigate (3+1)-dimensional systems which display a predominance of (1+1)-dimensional behavior in their physical properties. An example of this case can be some variants of the XY -model [51]. A possible extension of the studies performed in this paper could also be applied in the context of the generalized $O(N)$ nonlinear σ -model [52]. Another possibility would be to check if the large- N and ϵ -expansion predictions coincide since this comparison furnishes a typical non-trivial consistency check (see, e.g., Ref. [31]). Finally, we hope that the super-renormalizable model proposed here will motivate other authors to test their resummation techniques as well as non-perturbative methods (such as [1-3, 6-8, 53, 54]) in order to improve our seminal results.

A Evaluation of two loop diagrams with mixed propagators

Let us present some of the technical details for the evaluation of the Feynman diagrams and which have contribution from both fields, i.e., mixed propagators. Working in the $\overline{\text{MS}}$ dimensional regularization scheme, the setting sun like diagram, for instance, is

$$\begin{aligned}
 \text{---}\bullet\text{---}\overset{\curvearrowright}{\text{---}}\bullet\text{---}\text{---} &\equiv \Sigma_{\text{sun}}(p) \\
 &= -\frac{\lambda^2 N_j}{4} \left(\frac{\mu^2 e^{\gamma_E}}{4\pi} \right)^\epsilon \int_k \int_q \frac{1}{k^2 + m_i^2} \frac{1}{q^2 + m_j^2} \frac{1}{(p-k-q)^2 + m_j^2}. \quad (\text{A.1})
 \end{aligned}$$

Due to the structure of such diagram, the calculation in the coordinate space is simpler than in the momentum space [55, 56]. Writing the propagators in coordinate space,

$$G_i(x) \equiv \mathcal{F} \left\{ \frac{1}{l^2 + m_i^2} \right\} = \int_l \frac{e^{ilr}}{l^2 + m_i^2} = \frac{1}{(2\pi)^{\frac{D}{2}}} \left(\frac{r}{m_i} \right)^{1-\frac{D}{2}} K_{1-\frac{D}{2}}(m_i r), \quad (\text{A.2})$$

where $K_i(x)$ is the modified Bessel function of order i allows us to rewrite eq. (A.1) as

$$\Sigma_{\text{sun}}(p) = -\frac{\lambda^2 N_\chi}{4} \left(\frac{\mu^2 e^{\gamma_E}}{4\pi} \right)^\epsilon \int d^D r e^{ipr} G_j^2(x) G_i(x). \quad (\text{A.3})$$

Next, the angular integration in eq. (A.3) can be performed yielding

$$\int d^D r e^{ipr} = \frac{2\pi^{D/2}}{\Gamma(\frac{D}{2})} \int_0^\infty dr r^{D-1} {}_0F_1 \left(\frac{D}{2}, -\frac{p^2 r^2}{4} \right), \quad (\text{A.4})$$

with ${}_iF_j(a, b; c; z)$ representing the hypergeometric functions. Then, eq. (A.3) becomes

$$\begin{aligned} \Sigma_{\text{sun}}(p) = & -\frac{\lambda^2 N_j}{4} \left(\frac{\mu^2 e^{\gamma_E}}{4\pi} \right)^\varepsilon \frac{2^{1-\frac{D}{2}}}{(2\pi)^D \Gamma\left(\frac{D}{2}\right)} \frac{1}{m_j^{2-D} m_i^{1-\frac{D}{2}}} \\ & \times \int_0^\infty dr r^{2-\frac{D}{2}} {}_0F_1\left(\frac{D}{2}, -\frac{p^2 r^2}{4}\right) K_{1-\frac{D}{2}}^2(m_j r) K_{1-\frac{D}{2}}(m_i r). \end{aligned} \quad (\text{A.5})$$

Finally, by setting $D = 2 - 2\varepsilon$, taking the limit $\varepsilon \rightarrow 0$ and going on mass-shell, $p^2 = -m_i^2$, one obtains

$$\Sigma_{\text{sun}}(p) = -\frac{\lambda^2 N_\chi}{4(4\pi)^2 m_i m_j} \left[\pi^2 - 4 \tanh^{-1}\left(\frac{m_j}{m_i}\right) \ln\left(\frac{m_i}{m_j}\right) - \frac{m_j}{m_i} \Phi\left(\frac{m_j^2}{m_i^2}, 2, \frac{1}{2}\right) \right]. \quad (\text{A.6})$$

An analogous calculation can be used to obtain the other two-loop diagrams contributing to the pole masses and to the VEV, $\bar{\chi}$.

Acknowledgments

G.O.H. thanks Coordenação de Aperfeiçoamento de Pessoal de Nível Superior - (CAPES) - Finance Code 001, for a Ph.D. scholarship. M.B.P. is partially supported by Conselho Nacional de Desenvolvimento Científico e Tecnológico (CNPq), Grant No 307261/2021-2 and by CAPES - Finance Code 001. R.O.R. is partially supported by research grants from CNPq, Grant No. 307286/2021-5, and Fundação Carlos Chagas Filho de Amparo à Pesquisa do Estado do Rio de Janeiro (FAPERJ), Grant No. E-26/201.150/2021. This work has also been financed in part by Instituto Nacional de Ciência e Tecnologia de Física Nuclear e Aplicações (INCT-FNA), Process No. 464898/2014-5.

References

- [1] J. Häuser, W. Cassing, A. Peter, and M. Thoma, *Connected green function approach to symmetry breaking in ϕ 1+1 4-theory*, *Z. Phys. A* **353** (1995) 301, [[hep-ph/9408355](#)].
- [2] S. Rychkov and L. G. Vitale, *Hamiltonian truncation study of the ϕ^4 theory in two dimensions*, *Phys. Rev. D* **91** (2015) 085011, [[arXiv:1412.3460](#)].
- [3] M. Serone, G. Spada, and G. Villadoro, *$\lambda\phi^4$ Theory — Part I: The Symmetric Phase Beyond NNNNNNNLO*, *JHEP* **08** (2018) 148, [[arXiv:1805.05882](#)].
- [4] M. Serone, G. Spada, and G. Villadoro, *$\lambda\phi^4$ theory — Part II. The Broken Phase Beyond NNNN(NNNN)LO*, *JHEP* **05** (2019) 47, [[arXiv:1901.05023](#)].
- [5] P. Romatschke, *Simple non-perturbative resummation schemes beyond mean-field ii: Thermodynamics of scalar ϕ^4 theory in 1 + 1 dimensions at arbitrary coupling*, *Modern Physics Letters A* **35** (2020) 2050054, [[arXiv:1903.09661](#)].
- [6] P. Romatschke, *Simple non-perturbative resummation schemes beyond mean-field: case study for scalar ϕ^4 theory in 1+1 dimensions*, *JHEP* **03** (2019) 149, [[arXiv:1901.05483](#)].
- [7] D. Kadoh, Y. Kuramashi, Y. Nakamura, R. Sakai, S. Takeda, and Y. Yoshimura, *Tensor network analysis of critical coupling in two dimensional ϕ^4 theory*, *JHEP* **05** (2019) 184, [[arXiv:1811.12376](#)].

- [8] S. Bronzin, B. De Palma, and M. Guagnelli, *New monte carlo determination of the critical coupling in ϕ_2^4 theory*, *Phys. Rev. D* **99** (2019) 034508, [[arXiv:1807.03381](#)].
- [9] G. O. Heymans and M. B. Pinto, *Critical behavior of the 2d scalar theory: resumming the N⁸LO perturbative mass gap*, *JHEP* **07** (2021) 163, [[arXiv:2103.00354](#)].
- [10] B. Simon and R. B. Griffiths, *The $(\phi^4)_2$ Field Theory as a Classical Ising Model*, *Commun. Math. Phys.* **33** (1973) 145.
- [11] S.-J. Chang, *Existence of a second-order phase transition in a two-dimensional φ^4 field theory*, *Phys. Rev. D* **13** (1976) 2778.
- [12] S. Coleman, *There are no goldstone bosons in two dimensions*, *Commun. Math. Phys.* **31** (1973) 259.
- [13] N. D. Mermin and H. Wagner, *Absence of ferromagnetism or antiferromagnetism in one- or two-dimensional isotropic heisenberg models*, *Phys. Rev. Lett.* **17** (1966) 1133.
- [14] P. C. Hohenberg, *Existence of long-range order in one and two dimensions*, *Phys. Rev.* **158** (1967) 383.
- [15] L. D. Landau and E. M. Lifshitz, *Statistical Physics, Part 1*. Pergamon Press, Oxford, U.K., (1980).
- [16] J. M. Kosterlitz, D. R. Nelson, and M. E. Fisher, *Bicritical and tetracritical points in anisotropic antiferromagnetic systems*, *Phys. Rev. B* **13** (1976) 412.
- [17] P. Calabrese, A. Pelissetto, and E. Vicari, *Multicritical phenomena in $O(n_1) \oplus O(n_2)$ -symmetric theories*, *Phys. Rev. B* **67** (2003) 054505, [[cond-mat/0209580](#)].
- [18] A. Eichhorn, D. Mesterházy and M. M. Scherer, *Multicritical behavior in models with two competing order parameters*, *Phys. Rev. E* **88**, (2013) 042141, [[arXiv:1306.2952](#)].
- [19] E. Demler, W. Hanke, and S.-C. Zhang, *SO(5) theory of antiferromagnetism and superconductivity*, *Rev. Mod. Phys.* **76** (2004) 909, [[cond-mat/0405038](#)].
- [20] P. Meade and H. Ramani, *Unrestored electroweak symmetry*, *Phys. Rev. Lett.* **122** (2019) 041802, [[arXiv:1807.07578](#)].
- [21] I. Baldes and G. Servant, *High scale electroweak phase transition: baryogenesis \& symmetry non-restoration*, *JHEP* **10** (2018) 53, [[arXiv:1807.08770](#)].
- [22] O. Matsedonskyi and G. Servant, *High-temperature electroweak symmetry non-restoration from new fermions and implications for baryogenesis*, *JHEP* **09** (2020) 12, [[arXiv:2002.05174](#)].
- [23] O. Matsedonskyi, *High-temperature electroweak symmetry breaking by sm twins*, *JHEP* **04** (2021) 36, [[arXiv:2008.13725](#)].
- [24] B. Bajc, A. Lugo, and F. Sannino, *Asymptotically free and safe fate of symmetry nonrestoration*, *Phys. Rev. D* **103** (2021) 096014, [[arXiv:2012.08428](#)].
- [25] S. Chaudhuri and E. Rabinovici, *Thermal order in large n conformal gauge theories*, *JHEP* **04** (2021) 203, [[arXiv:2011.13981](#)].
- [26] S. Chaudhuri and E. Rabinovici, *Symmetry breaking at high temperatures in large n gauge theories*, *JHEP* **08** (2021) 148, [[arXiv:2011.13981](#)].
- [27] L. Niemi, P. Schicho, and T. V. I. Tenkanen, *Singlet-assisted electroweak phase transition at two loops*, *Phys. Rev. D* **103** (2021) 115035, [[arXiv:2103.07467](#)].

- [28] D. G. S. Ramazanov, E. Babichev and A. Vikman, *Singlet-assisted electroweak phase transition at two loops*, *Phys. Rev. D* **103** (2021) 115035, [[arXiv:2104.13722](#)].
- [29] S. Weinberg, *Gauge and global symmetries at high temperature*, *Phys. Rev. D* **9** (1974) 3357.
- [30] N. Chai, A. Dymarsky, and M. Smolkin, *Model of persistent breaking of discrete symmetry*, *Phys. Rev. Lett.* **128** (2022) 011601, [[arXiv:2106.09723](#)].
- [31] N. Chai, S. Chaudhuri, C. Choi, Z. Komargodski, E. Rabinovici, and M. Smolkin, *Thermal order in conformal theories*, *Phys. Rev. D* **102** (2020) 065014, [[arXiv:2005.03676](#)].
- [32] N. Chai, S. Chaudhuri, C. Choi, Z. Komargodski, E. Rabinovici, and M. Smolkin, *Symmetry breaking at all temperatures*, *Phys. Rev. Lett.* **125** (2020) 131603.
- [33] G. Delfino and N. Lamsen, *Critical points of coupled vector-Ising systems. Exact results*, *J. Phys. A: Math. Theor.* **52** (2019) 35LT02, [[arXiv:1902.09901](#)].
- [34] R. N. Mohapatra and G. Senjanović, *Soft CP-invariance violation at high temperature*, *Phys. Rev. Lett.* **42** (1979) 1651.
- [35] K. Klimenko, *Gaussian effective potential and symmetry restoration at high temperatures in four-dimensional $O(N) \times O(N)$ field theory*, *Z. Phys. C* **43** (1989), no. 4 581.
- [36] G. Bimonte and G. Lozano, *Can symmetry non-restoration solve the monopole problem?*, *Nucl. Phys. B* **460** (1996) 155.
- [37] G. Amelino-Camelia, *On the cjt formalism in multi-field theories*, *Nuclear Physics B* **476** (1996) 255, [[hep-th/9603135](#)].
- [38] J. Orloff, *The w price for symmetry non-restoration*, *Phys. Lett. B* **403** (1997) 309, [[hep-ph/9611398](#)].
- [39] T. G. Roos, *Wilson renormalization group study of inverse symmetry breaking*, *Phys. Rev. D* **54** (1996) 2944, [[hep-th/9511073](#)].
- [40] K. Jansen and M. Laine, *Inverse symmetry breaking with 4d lattice simulations*, *Phys. Lett. B* **435** (1998) 166, [[hep-lat/9805024](#)].
- [41] G. Bimonte, D. Iñiguez, A. Tarancón, and C. Ullod, *Inverse symmetry breaking on the lattice: an accurate mc study*, *Nuclear Physics B* **559** (1999) 103, [[hep-lat/9903027](#)].
- [42] M. B. Pinto and R. O. Ramos, *Nonperturbative study of inverse symmetry breaking at high temperatures*, *Phys. Rev. D* **61** (2000) 125016, [[hep-ph/9912273](#)].
- [43] M. B. Pinto, R. O. Ramos, and J. E. Parreira, *Phase transition patterns in relativistic and nonrelativistic multi-scalar-field models*, *Phys. Rev. D* **71** (2005) 123519, [[hep-th/0506131](#)].
- [44] M. B. Pinto and R. O. Ramos, *Inverse symmetry breaking in multi-scalar field theories*, *Jour. of Phys. A* **39** (2006) 6649, [[cond-mat/0605508](#)].
- [45] R. L. S. Farias, R. O. Ramos, and D. S. Rosa, *Symmetry breaking patterns for two coupled complex scalar fields at finite temperature and in an external magnetic field*, *Phys. Rev. D* **104** (2021) 096011, [[arXiv:2109.03671](#)].
- [46] I. S. Gradshteyn and I. M. Ryzhik, *Tables of Integrals, Series, and Products*. Academic Press, San Diego, U.S.A., 6 ed., (2000).
- [47] S. Coleman, R. Jackiw, and H. D. Politzer, *Spontaneous symmetry breaking in the $O(N)$ model for large N* , *Phys. Rev. D* **10** (1974) 2491.

- [48] D. J. Gross and A. Neveu, *Dynamical symmetry breaking in asymptotically free field theories*, *Phys. Rev. D* **10** (1974) 3235.
- [49] V. L. Berezinsky, *Destruction of Long-range Order in One-dimensional and Two-dimensional Systems Possessing a Continuous Symmetry Group. II. Quantum Systems.*, *Sov. Phys. JETP* **34** (1972) 610.
- [50] J. M. Kosterlitz and D. J. Thouless, *Ordering, metastability and phase transitions in two-dimensional systems*, *Jour. of Phys. C* **6** (1973) 1181.
- [51] J. P. de Lima and L. L. Gonçalves, *The XY model on the one-dimensional superlattice: static properties*, *J. Magn. Magn. Mater.* **206**, (1999) 135, [[cond-mat/991065](#)].
- [52] T. Banerjee, N. Sarkar and A. Basu, *Phase transitions and order in two-dimensional generalized nonlinear σ models*, *Phys. Rev. E* **92** (2015) 062133, [[arXiv:1508.02214](#)].
- [53] T. Cohen, K. Farnsworth, R. Houtz and M. A. Luty, *Hamiltonian Truncation Effective Theory*, [[arXiv:2110.08273](#)].
- [54] S. S. Chabysheva and J. R. Hiller, *Tadpoles and vacuum bubbles in light-front quantization*, [[arXiv:2201.00123](#)].
- [55] J. C. Collins, *Renormalization*. Cambridge Univ. Press, Cambridge, U.K., (1984).
- [56] E. Braaten and A. Nieto, *Effective field theory approach to high-temperature thermodynamics*, *Phys. Rev. D* **51** (1995) 6990, [[hep-ph/9501375](#)].